

Tactical Rewind: Self-Correction via Backtracking in Vision-and-Language Navigation

Liyiming Ke* Xiujun Li*† Yonatan Bisk* Ari Holtzman* Zhe Gan†
Jingjing Liu† Jianfeng Gao† Yejin Choi*‡ Siddhartha Srinivasa*
*Paul G. Allen School of Computer Science & Engineering, University of Washington
†Microsoft Research AI ‡Allen Institute for Artificial Intelligence
{kayke, xiujun, ybisk, ahai, yejin, sid dh}@cs.washington.edu
{zhgan, jingjl, jfgao}@microsoft.com

Abstract

We present FAST NAVIGATOR, a general framework for action decoding, which yields state-of-the-art results on the recent Room-to-Room (R2R) Vision-and-Language navigation challenge of Anderson et. al. (2018). Given a natural language instruction and photo-realistic image views of a previously unseen environment, the agent must navigate from a source to a target location as quickly as possible. While all of current approaches make local action decisions or score entire trajectories with beam search, our framework seamlessly balances local and global signals when exploring the environment. Importantly, this allows us to act greedily, but use global signals to backtrack when necessary. Our FAST framework, applied to existing models, yielded a 17% relative gain over the previous state-of-the-art, an absolute 6% gain on success rate weighted by path length (SPL).¹

1. Introduction

When a person reads an instruction like “Exit the bathroom, take the door on your right and pass the sofa.”, she builds a virtual map which includes landmarks (Have I gone through a second door yet?) and a marker of success (Did I reach the top of the stairs?). Training an embodied agent to accomplish such a task with only access to ego-centric vision and individually supervised actions requires building rich multi-modal representations from limited data [2].

Most current approaches to Vision-and-Language Navigation (VLN) cast the task using the seq2seq (or encoder-decoder) framework [21] where language and vision are encoded as the input and an ideal action sequence is decoded as the output. In addition to the original work introduc-

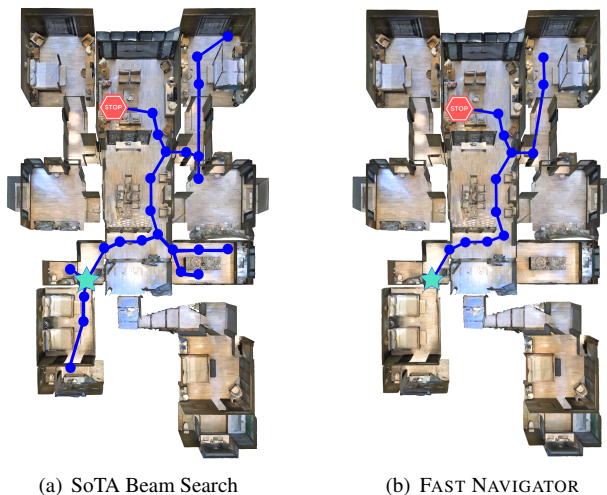


Figure 1. Top-down view of the trajectory graphs between beam search agent and FAST. Blue star is the start, Red stop is the target.

ing VLN, several subsequent architectures also fall into this framing, though with important advances in attention mechanisms, global scoring, and beam search [2, 13, 10].

Inherent to the seq2seq formulation is the problem of *exposure bias* [19], wherein a model that has only been trained to predict one-step into the future based on the ground-truth sequence is incapable of performing accurately using its own self-generated sequence. Previous work with seq2seq models have attempted to address this bias with student-forcing and beam search.

Student-forcing exposes the model to its own prediction during training, teaching the agent how to recover. However, once the agent has deviated from the correct path, even though we can calculate the shortest path to the target, the original instruction no longer applies. This makes student-forcing only a partial solution. In the Supplementary Materials (§A.1), we show that student-forcing cannot

¹The code is available at <https://github.com/Kelym/FAST>.

completely solve the exposure bias problem, and the agent falls in loops when confused.

Beam search, at the other extreme, builds global trajectories to score and incurs a cost proportional to the number of rollouts, which is often prohibitively high. This is fundamentally at odds with the goal of building an agent that efficiently navigates an environment. Nobody wants to deploy a household robot that re-navigates the entire house 100 times² before executing each command, even if they ultimately get to the right place. Table 1 shows the top performing systems on the VLN leaderboard³, all require broad exploration that yield long trajectories which results in poor SPL performance (Success weighted by Path Length [1]).

To fix the issues of exposure bias and expensive beam-search decoding, we propose the FAST NAVIGATOR⁴ which enables agents to *compare partial paths with different lengths* based on local and global information and backtrack when making a mistake. Figure 1 illustrates the trajectory graphs created by the current published state-of-the-art (SoTA) agent versus our own.

Our method is a form of asynchronous search, enabling us to combine global and local knowledge to score and compare (partial) trajectories of different lengths. We evaluate our progress to the goal, by modeling how closely our previous actions align with the given text instructions. Our framework achieves this via a *fusion* function which converts local action knowledge and history into an estimated score of progress, and this score determines what greedy local action to take and if the agent should backtrack to a previous location. The primary contribution of our work is to marry neural decoding with traditional approaches to search. This insight brings significant gains across the board to existing models.

2. Method

The VLN task requires an agent to carry out a natural language instruction in a photo-realistic environment. The agent is provided with instruction \mathcal{X} that is composed of several sentences describing a desired trajectory. At each step t the agent observes its surroundings \mathcal{V}_t . Because the agent can look around, \mathcal{V}_t is actually a set of $K = 36$ different views. We denote each view as \mathcal{V}_t^k . Given this multimodal input, the agent is trained to execute a sequence of actions $a_1, a_2, \dots, a_T \in \mathcal{A}$ to reach the target location. Following recent work [13, 10], we use a panoramic action space where each action corresponds to moving towards one of the K views, in lieu of R2R’s original primitive action space (i.e. *left*, *right*, etc) [2, 23]. In addition, this formu-

²This is calculated based on the length of SPEAKER-FOLLOWER agent paths and human paths on the R2R dataset.

³<https://evalai.cloudcv.org/web/challenges/challenge-page/97/leaderboard/270>

⁴FAST stands for Frontier Aware Search with backTracking.

lation also includes a *stop* action to indicate the agent has reached the goal.

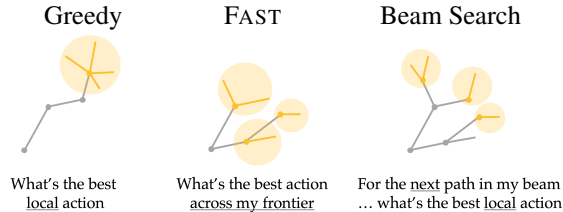


Figure 2. All VLN agents are performing search. The orange areas highlight the frontier for different navigation methods.

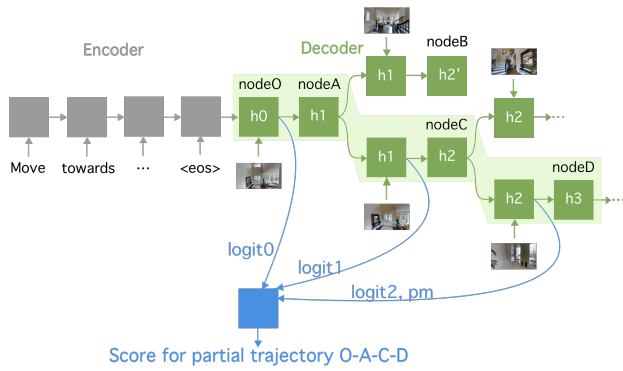
2.1. Learning Signals

Key to progress in visual navigation is that *all* VLN approaches are performing search (Figure 2). Current work often falls into one of two extremes: using only local information as with Greedy Decoding, or by fully sweeping multiple paths simultaneously as with Beam Search. To build an agent to navigate in an environment successfully and efficiently, we leverage both *Local* and *Global* information, to enable the agent to make a local decision while being aware of the global progress, and also efficiently backtrack when the agent makes a mistake. Inspired by previous work [10, 13], there are three learning signals in our work:

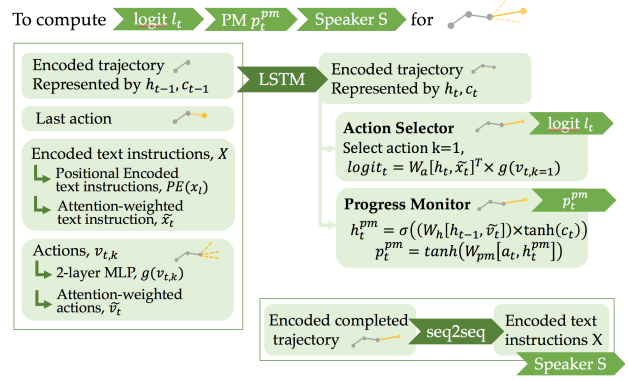
LOGIT l_t : is a kind of local information at each time step. Specifically, the original language instruction is encoded via an LSTM, and another LSTM as a decoder with an attention mechanism to generate a sequence of actions. At each time step t of decoding, a distribution over actions (logits) is produced by taking the the dot product of the decoder hidden state which each candidate action a_t^i . The logit of the action chosen at time t is denoted l_t .

PM p_t^{pm} : is a kind of global information. It (Progress Monitor) tracks how much of the instruction has been completed [13]. Formally, the model uses the (decoder) LSTM’s current cell state c_t , previous hidden state h_{t-1} , visual inputs \mathcal{V}_t , and attention over the language embeddings α_t to compute a score p_t^{pm} that ranges between $[-1, 1]$ and indicates the agent’s normalized progress. Training this indicator provides a regularizing effect on the attention alignments, helping the model learn language-to-vision correspondences which can be used to compare multiple trajectories.

SPEAKER S : is a kind of global information. Given a sequence of visual observations and actions, we can train a seq2seq captioning model to produce a textual description (as a “speaker” [10]). It provides two benefits: 1) New trajectories in the environment can be automatically annotated with the synthetic instructions by the “speaker”. 2) The “speaker” can score the likelihood that a given trajectory corresponds to the original instruction. Important for our work, it introduces a new global scoring mechanism.



(a) Instructions and visual observations are encoded as hidden vectors tracing out multiple paths through the world. These vectors can then be accumulated to score a sequence of actions, see an example of partial trajectory O-A-C-D.



(b) At each time step, the predicted action sequence and visual observation are attended to the encoded instruction, to produce the logits for next action, and also a process monitor score.

Figure 3. (a). Show how the three signals are extracted from the partial trajectory in a seq2seq framework of VLN; (b). Show how to produce the three signals.

2.2. Framework

We introduce an extendable framework⁵ which integrates the above three signals (l_t , p_t^{pm} , S)⁶ and trains new indicators to equip the agent with these capabilities at any point:

1. Should we backtrack?
2. Where should we backtrack?
3. Which visited node is most likely to be the goal?
4. When do we terminate search?

These questions pertain to all existing approaches. In particular, greedy approaches never backtrack and do not compare partial trajectories, while global beam search techniques always backtrack but end up wasting efforts. By taking a more principled approach to modeling navigation as graph traversal, our framework allows for nuanced and adaptive answers to each of these questions.

For navigation, the graph is defined by a series of locations in the house, “nodes”. For each task, the agent is placed at a starting node and the agent’s movement in the house creates a trajectory comprised of a sequence of $\langle \text{node } u, \text{action } a \rangle$ pairs. We denote a *partial* trajectory up to time t as τ_t , or colloquially, the set of physical locations visited and the action taken at each point:

$$\tau_t = \{(u_i, a_i)\}_{i=1}^t \quad (1)$$

For any partial trajectory, the last action is *proposed* and evaluated, but they are not *executed*. Instead, the model

⁵Figure 3(a) exemplifies how to integrate the three signals in a seq2seq framework.

⁶Figure 3(b) shows how to compute the three signals.

will choose whether to expand a partial trajectory or execute a *stop* action to complete the trajectory. Importantly, this means every node visited by the agent can serve as a possible final destination. The agent moves in the environment by choosing to extend a partial trajectory: moving to the last node of the partial trajectory and executing its last action. Once the agent executes the last action and arrives at a new node, it then realizes the actions available at the new node and collects them to make a set of new partial trajectories.

At each time step, the agent has to i) remember the set of partial trajectories it has not expanded, ii) remember the completed trajectories that might be the candidate path, iii) calculate the accumulated cost of partial trajectories and the expected gain of its proposed action and iv) compares all partial trajectories.

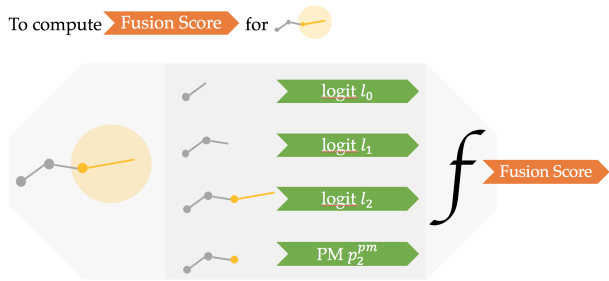
For this purpose, we maintain two priority queues: a frontier queue Q_F for partial trajectories and a global candidate queue Q_C for completed trajectories. The two priority queues are sorted by local \mathcal{L} and global \mathcal{G} scores respectively: \mathcal{L} scores the quality of all partial trajectories with their proposed actions and maintains their order in frontier queue Q_F ; \mathcal{G} scores the quality of completed trajectories and maintains the order in the candidate queue Q_C .

In the experiment section (§4.3), we will explore alternative formula for \mathcal{L} and \mathcal{G} . To give you an example, we define \mathcal{L} and \mathcal{G} using the signals described in §2.1 and a function f which is implemented as a neural network.

$$\mathcal{L} \leftarrow \sum_{0 \rightarrow t} l_i \quad (2)$$

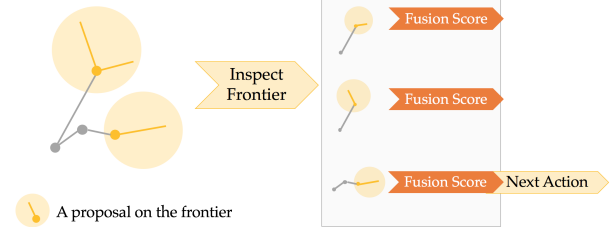
$$\mathcal{G} \leftarrow f(S, p_t^{pm}, \sum_{0 \rightarrow t} l_i, \dots) \quad (3)$$

To allow the agent to efficiently navigate and follow the instruction, we use an approximation of D* search. FAST



(a) Both the local \mathcal{L} and global \mathcal{G} scores can be trained to condition on arbitrary information. Here we show the fusion of historical logits and a progress monitor into a single score.

As FAST is running ...



(b) Expansion queue maintains all possible next actions from all partial trajectories. The options are sorted by their scores (Figure 4(a)) in order to select the next action.

Figure 4. Arbitrary signals can be computed from partial trajectories to learn a scoring function (left) which ranks all possible actions in our expansion queue (right). This provides a flexible and extendable framework for optimal action decoding.

expands its optimal partial trajectory until it decides to backtrack (**Q1**). It decides on where to backtrack (**Q2**) by ranking all partial trajectories. Finally, to propose the final goal location (**Q3 & Q4**), the agent ranks the completed global trajectories in the candidate queue \mathcal{Q}_C . We explain these components in more detail below.

Q1: Should we backtrack? When an agent makes a mistake or gets lost, backtracking allows it to move to a more promising partial trajectory, however retracing your steps increases the length of the final path. To determine when it is worth incurring the costly backtracking, we proposed two simple strategies: *Explore* and *Exploit*.

- *Explore* always backtracks to the most promising partial trajectory. This approach is similar to beam search, but rather than simply moving to the next partial trajectory in the beam, the agent computes the most promising node to backtrack to (**Q2**).
- *Exploit*, in contrast, commits to the current partial trajectory, always executing the best action available at the agent’s current location. This approach is similar to greedy decoding, except that we will backtrack when the agent is confused (i.e. when the best local action leads the agent to revisit a node, creating a loop, see the SMNA examples in Supplementary Materials §A.1).

Q2: Where should we backtrack? Making this decision involves using \mathcal{L} to score all partial trajectories. Intuitively, the better a partial trajectory aligns with the given description, the higher the value of \mathcal{L} . Thus, if we can assume the veracity of \mathcal{L} we simply return to the highest scoring node when backtracking. Throughout our paper we explore several functions for computing \mathcal{L} , but present two simple techniques here, each acting over the sequence of actions that comprise a trajectory:

Sum-of-log $\sum_{0 \rightarrow t} \log p_i$ One simple approach is to sum the log-probabilities of every previous action, thereby computing the probability of a partial trajectory.

Sum-of-logits $\sum_{0 \rightarrow t} l_i$ We found that summing the unnormalized logits of previous actions performs better than using probabilities. These values are computed via an attention mechanism between the hidden state, observations and language. In this way, their magnitude captures how well the action was aligned with the target description (information that is lost during normalization).⁷

Finally during exploration, the agent implicitly constructs a “mental map” of the world. This allows us to make search more efficient by refusing to revisit nodes, unless they lead to a high value unexplored path.

Q3: Which visited node is most likely to be the goal? Different from the existing approaches, FAST considers every point that the agent has visited as a candidate for the final destination,⁸ meaning we must rerank all candidates. We achieve this with \mathcal{G} , a trainable neural network function to incorporate all global information for each candidate and ranks them accordingly. A simple visualization is shown in Figure 4(a).

We experiment several approaches to compute \mathcal{G} , which integrates \mathcal{L} , the progress monitor, speaker score and a trainable ensemble (§4.3).

Q4: When to terminate the search? It is easy to see that FAST can cover both the greedy decoding and beam search

⁷This is particularly problematic when an agent is lost as many low-value logits can still yield a comparatively high probability (e.g. uniform or random). We also experiment with variations on these approaches (e.g. means instead of sums) in §4.

⁸There can be more than one trajectory connecting the starting node to each visited node.

framework. In addition, we define two alternative stopping criterion for FAST:

- When a partial trajectory decides to terminate.
- When we have expanded M nodes. In §3 we ablate the effect of choosing different M .

2.3. Algorithm

Here we present the algorithm flow of our FAST framework. When the agent is initialized and placed on the starting node, both the candidate and frontier queues are empty. The agent then adds all possible next actions to the frontier queue; and adds its current location to the candidate queue:

$$Q_F \leftarrow Q_F + \forall_{i \in K} \{\tau_0 \cup (u_0, a_i)\} \quad (4)$$

$$Q_C \leftarrow Q_C + \tau_0 \quad (5)$$

Now that the Q_F is not empty and the stop criterion is not met, we choose the best partial trajectory from the frontier queue under the local scoring function:

$$\hat{\tau} \leftarrow \arg \max_{\tau_i} \mathcal{L}(Q_F) \quad (6)$$

Following $\hat{\tau}$, we perform the final action proposal a_t to move to a new node (location in the house). We can now update our candidate queue with this location and our frontier queue with all possible new actions. We then either continue by exploiting the available actions at the new location or backtrack, depending on the choice of backtrack criterion. We repeat this process until the model chooses to stop and returns the best candidate trajectory.

$$\tau^* \leftarrow \arg \max_{\tau} \mathcal{G}(Q_C) \quad (7)$$

Algorithm 1 more precisely outlines the full procedure for our approach. §4.3 details the different approaches to scoring partial and complete trajectories.

3. Experiments

We evaluate our approach with the VLN Room-to-Room (R2R) dataset [2]. At the beginning of the task, the agent is provided a natural language instruction and a specific start location in the environment, the job of the agent is to navigate to the target location specified in the instruction as fast as possible. R2R is built upon the Matterport3D dataset [5], which consists of >194K images, yielding 10,800 panoramic views (“nodes”) and 7,189 paths. Each path is paired with three natural language instructions.

3.1. Metrics

We evaluate our approach on all the metrics available to the R2R dataset:

TL Trajectory Length: The average length of the navigation trajectory.

Algorithm 1 FAST NAVIGATOR

```

1: procedure FAST NAVIGATOR
2:    $Q_F^{sort=\mathcal{L}}, Q_C^{sort=\mathcal{G}} = \{\}, \{\}$ 
3:    $Q_F \leftarrow (u_0, a_0 = \text{None})$  ▷ Initial Proposal
4:    $\hat{\tau} \leftarrow \emptyset$ 
5:    $M \leftarrow \emptyset$  ▷ Mental Map
6:   while  $Q_F \neq \emptyset$  and stop criterion do
7:     if need backtrack or  $\hat{\tau} == \emptyset$  then
8:        $\hat{\tau} \leftarrow Q_F.\text{pop}$ 
9:     end if
10:     $\hat{u}_{t-1}, \hat{a}_{t-1} \leftarrow \hat{\tau}.\text{last}$ 
11:    if  $(\hat{u}_{t-1}, \hat{a}_{t-1}) \in M$  then
12:       $u_t \leftarrow M(\hat{u}_{t-1}, \hat{a}_{t-1})$ 
13:    else
14:       $u_t \leftarrow \text{move to } u_{t-1} \text{ and execute } a_{t-1}$ 
15:       $M(\hat{u}_{t-1}, \hat{a}_{t-1}) \leftarrow u_t$ 
16:    end if
17:    for  $a_k$  in best  $K$  next actions do
18:       $Q_F \leftarrow Q_F \cup \{\hat{\tau} + (u_t, a_k)\}$ 
19:    end for
20:     $Q_C \leftarrow Q_C \cup \hat{\tau}$ 
21:     $\hat{\tau} \leftarrow \hat{\tau} + (u_t, a^*)$  where  $a^*$  is the best action
22:  end while
23:  return  $Q_C.\text{pop}$ 
24: end procedure

```

NE Navigation Error: The mean of the shortest path distance in meters between the agent’s final location and the goal location.

SR Success Rate: The percentage of the agent’s final location is less than 3 meters away from the goal location.

SPL Success weighted by Path Length: A metric that trades-offs SR against TL [1]. Higher is better.

3.2. Baselines

We compare to several published baselines on this task.⁹

- **RANDOM:** is an agent that randomly selects a direction and heads in that direction for five steps [2].
- **SEQ2SEQ:** is the best performing model in the R2R dataset paper [2].
- **SPEAKER-FOLLOWER** [10]: is an agent trained with data augmentation from a speaker model on the panoramic action space.
- **SMNA** [13]: is an agent trained with visual-textual co-grounding module and a progress monitor on the panoramic action space.¹⁰

Model	Validation Seen				Validation Unseen				Test Unseen				
	TL	NE	SR	SPL	TL	NE	SR	SPL	TL	NE	SR	SPL	
RANDOM	9.58	9.45	0.16	-	9.77	9.23	0.16	-	9.93	9.77	0.13	0.12	
Seq2seq	11.33	6.01	0.39	-	8.39	7.81	0.22	-	8.13	7.85	0.20	0.18	
Our baseline	11.69	3.31	0.69	0.63	12.61	5.48	0.47	0.41	-	-	-	-	
Greedy	SMNA	-	-	-	-	-	-	-	18.04	5.67	0.48	0.35	
	SPEAKER-FOLLOWER	-	-	-	-	-	-	-	14.82	6.62	0.35	0.28	
	+ FAST (short)	-	-	-	-	21.17	4.97	0.56	0.43	22.08	5.14	0.54	0.41
Beam	SMNA	-	3.23	0.70	-	-	5.04	0.57	-	373.09	4.48	0.61	0.02
	SPEAKER-FOLLOWER	-	3.88	0.63	-	-	5.24	0.50	-	1,257.30	4.87	0.53	0.01
	+ FAST (long)	188.06	3.13	0.70	0.04	224.42	4.03	0.63	0.02	196.53	4.29	0.61	0.03
Human	-	-	-	-	-	-	-	-	11.85	1.61	0.86	0.76	

Table 1. Our results and SMNA re-implementation are shown in gray highlighted rows. **Bolding** indicates the best value per section and **blue** indicates best values overall. We include both a short and long version of our approach to compare to existing models greedy and beam search approaches.

3.3. Results

Plug-n-Play A key benefit of our technique is the simple nature of integrating it with current approaches for dramatic gains in performance. In Table 2, we show how the simple sum-of-logits fusion method enhances the two previously best performing models. By simply changing their greedy decoders to FAST with no global information and therefore no reranking, we see immediate gains of 6 and 9 points in success rate for SPEAKER-FOLLOWER and SMNA, respectively. Due to the models’ new ability to backtrack, the trajectory lengths increase slightly, however the increase in success rate is so great that SPL increases as well.

Validation Unseen	SR (%)	SPL (%)	TL
SPEAKER-FOLLOWER	37	28	15.32
+ FAST	43 (+6)	29 (+1)	20.63
SMNA	47	41	12.61
+ FAST	56 (+9)	43 (+2)	21.17

Table 2. Plug-n-play performance gains achieved by adding FAST to current SoTA models.

In Table 1 we perform a complete performance comparison against published numbers and settings for existing models. Here we report performance of our model using local information from the SMNA agent. Our FAST agents use a simple sum of logits *fusion* method to compute \mathcal{L} . The FAST (short) agent uses our exploit strategy to determine when to backtrack and terminate the search when the best local action proposes to stop. In contrast, the FAST

⁹Some baselines on the leaderboard are not public yet, therefore we cannot compare with them directly on the training and validation sets.

¹⁰Our implementation of the SMNA model matches published validation numbers. All of our experiments are based on full re-implementations.

(long) agent trains a neural network reranker \mathcal{G} that incorporates the logits, the progress monitor of SMNA and the SPEAKER model from SPEAKER-FOLLOWER into a single score. This agent terminates after expanding 55 nodes. Our approach dramatically outperforms the existing model in terms of efficiency, matching the best overall success despite taking 150 - 1,000 fewer steps. This efficiency gain shows up in the SPL metric where we outperform previous approaches in every setting.¹¹

We have interspersed our FAST (short) and FAST (long) results in the Greedy and Beam Search sections of the table for ease of comparison. We see that our short trajectory model dramatically outperforms current approaches in success rate and SPL, achieving a state-of-the-art of 0.41. If we allow our agent to continue exploring to match existing peak success rates, we do so in half the time (196 vs 373).

4. Analysis

Throughout the analysis we isolate the effects of local and global knowledge, the importance of backtracking, and various stopping criteria. In addition, we include three qualitative intuitive examples to illustrate the model’s behavior in the Supplementary Materials (§A.1). We are able to perform such an analysis because our approach has access to the same information as previous architectures, but is dramatically more efficient. Our claims and results are general and our FAST approach should benefit future architectures in VLN.

4.1. Fixing Your Mistakes

To investigate how much models benefit from backtracking, Figure 5 plots a model’s likelihood to successfully com-

¹¹An ablation of these choices is presented in §4.

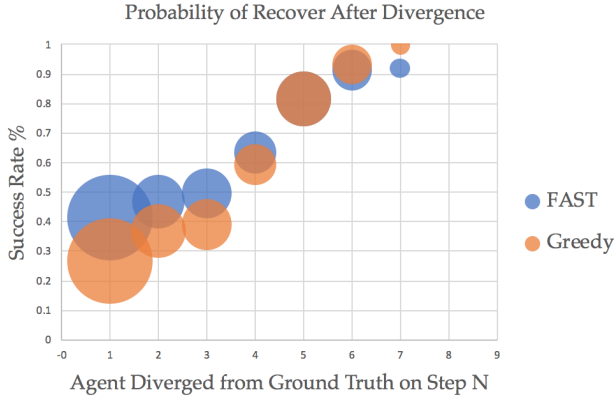


Figure 5. The size of the circles is representative of what percentage of agents diverge on step = N. We show that FAST is able to recover from early divergences off of the ground-truth, and that most divergences happen early on.

plete the task after making a mistake at each different step. Here we use SMNA as our greedy baseline. Our analysis finds that the previous SoTA model makes a mistake at the very first action 40% of the time. In Figure 5, we allow us to look up the effect of this error. In particular, we see that if their greedy approach makes a mistake at its first action, it has a <30% chance of successfully completing the task. In contrast, because FAST detects its mistake, it returns to the starting position and tries again. This simple one-step backtracking increases the likelihood of success by over 10%. In fact, the greedy approach is only equally successful if it makes it over halfway through the instruction without a mistake.

4.2. Knowing When To Stop Exploring

The stopping criterion balances exploration and exploitation. Unlike previous approaches, our framework allows us to compare different criteria and gives us the flexibility to determine which one is right for a given domain. The best available stopping criterion for VLN is not necessarily the best in general. We investigated the number of nodes to expand before terminating the algorithm and plot the resulting success rate and SPL in Figure 6. One important finding is that the model success rate, though increasing with more nodes expanded, does not match the oracle rate, i.e. as the agent expands 40 nodes, it has visited the true target node over 90% of the time but cannot recognize as the final destination. This motivates an analysis of the utility of our global information and whether it is truly predictive (Table 4), which we will investigate in §4.3.

4.3. Local and Global Scoring

Following §2.3, core to our approach are two queues: Frontier Queue for expansion and Candidate Queue for

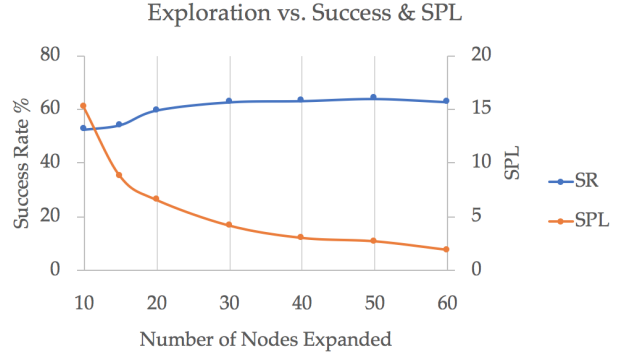


Figure 6. The expected success goes up with the number of nodes explored, before plateauing, while SPL (which is extremely sensitive to length) continually decreases with added exploration.

proposing the final candidate. Each queue can use arbitrary information for scoring (partial) trajectories. We compare the effects of combing different set of signals for scoring each queue.

Fusion Methods for scoring partial trajectories An ideal model would include as much global information as possible when scoring partial trajectories in the frontier expansion queue. Thus we investigated several sources of pseudo-global information and ten different ways to combine them. The first four use only local information while the rest attempts to fuse local and global information.

The top half of Table 3 shows the performance when only considering local information providers. For example, the third row of the table shows that summing the logit scores of nodes along the partial trajectory as the \mathcal{L} score for that trajectory achieves an SPL score of 44.74. Note that though all information originates with the same hidden vectors, what values are computed and how they are aggregated has a substantial effect on performance. Overall, we find that summing unnormalized logits performs the best considering its outstanding SR and above average SPL. This implies there is important activation information present in the networks outputs which is being thrown away by normalization and therefore discarded by other techniques.

The bottom of Table 3 explores potential ways to combine information from both local and global providers. These are motivated by beam-rescoring techniques in previous work (e.g. multiplying by the progress monitor). Correctly integrating signals is challenging, in part due to differences in scale. For example, the logit is unbounded (+/-), log probabilities are unbounded in the negative and the progress monitor is confined to a score between -1 and 1. Direct integration of the progress monitor unfortunately did not yield promising results, but future signals may be more powerful.

		Validation		
Heur/step	Combine	SR	SPL	Len
logit	mean	53.89	44.74	14.80
log prob	mean	53.85	44.14	15.57
logit	sum	56.66	43.64	21.17
log prob	sum	56.23	42.66	21.70
logit	mean / pm	51.21	43.81	12.94
log prob	mean / pm	51.68	44.17	12.55
logit	mean * pm	52.83	41.81	20.9
log prob	mean * pm	54.02	41.42	22.23
logit	sum * pm	50.95	41.28	20.25
log prob	sum * pm	50.95	40.44	22.42

Table 3. Performance of different fusion methods for scoring partial trajectories.

Fusion methods for ranking complete trajectories Previous work [10] used state-factored beam search to generate M candidates and rank the complete trajectories using probability of speaker and follower scores $\operatorname{argmax}_{r \in R(d)} P_S(d|r)^\lambda * P_F(d|r)^{(1-\lambda)}$. In addition to the speaker score and progress monitor score used by previous models, we also experiment with using \mathcal{L} in computing \mathcal{G} . To inspect the performance of using different fusion methods, we run FAST NAVIGATOR to expand 40 nodes on the frontier and collect candidate trajectories. Table 4 shows the performance of different fusion scores to rank the complete trajectories. Unfortunately, we see that most techniques have a limited understanding of the global task goal and formulation. We do however find a significant improvement on unseen trajectories when all signals are combined. To accomplish this we train a multi-layer perceptron to aggregate and weight our predictors. It is important to note that any improvement that can be made to the underlying models or new features introduced by future work will directly correlate to gains in this component of the pipeline.

The top line of Table 4, shows the oracle performance. This indicates how far current global information providers have yet to go. Closing this gap is an important direction for future work.

4.4. Intuitive Behavior

In the Supplementary Materials (§A.1), we provide three real examples to show how our model performs when compared to greedy decoding (SMNA model). It highlights how the same observations lead to drastically different behavior during an agent’s rollout. Specifically, in Figure A1 and Figure A2, the greedy decoder is forced into a behavioral loop, because only local improvements are considered. Using FAST, it clearly shows that even a single backtracking step can break the agent out of poor behavioral choices.

	Train	Val Seen	Val Unseen
<i>Oracle</i>	99.13	92.85	90.20
Σl_i	78.78	62.49	56.49
μl_i	85.78	66.99	54.41
Σp_i	91.25	68.56	56.15
μp_i	91.60	69.34	58.75
p_t^{pm}	66.71	53.67	50.15
\mathcal{S}	69.99	53.77	43.68
<i>All</i>	90.16	71.00	64.03

Table 4. Success Rate using seven different fusion scores as \mathcal{G} to rerank the destination node from the candidate pool.

5. Related Work

Our work focuses on and complements recent advances in Vision-and-Language Navigation (VLN) as introduced by [2], but many aspects of the task and core technologies date much further back. The natural language community has explored instruction following with 2D maps [17, 14] and more recently computer-rendered 3D environments [16]. Due to the enormous visual complexity of real world scenes, the literature surrounding VLN also builds off of computer vision work in referring expressions [15, 24], visual question answering [3], and most recently ego-centric QA that requires navigation to answer questions [11, 8, 9]. Finally, core to the work we present here is the field of search that dates back to the earliest days of AI [18, 20], while being largely absent from recent literature on VLN, which tends to focus more on neural architecture design.

Alongside the Room-to-Room dataset, [2] introduced a seq2seq model trained with “student-forcing”. Later work then integrated a planning module that combined model-based and model-free reinforcement learning techniques to better generalize to unseen environments [23], and a cross-modal matching method that enforces cross-modal grounding both locally and globally via reinforcement learning [22]. Two substantial improvements came in the form of a panoramic action space and training a “speaker” model to enable data augmentation and trajectory reranking for beam search [10]. Most recently, [13] leverages a visual-textual co-grounding attention mechanism to better align the instruction and visual scenes, and incorporates a progress monitor to estimate the agent’s current progress towards the goal. This approach still requires beam search for peak performance. A side effect of beam search techniques is that they lead to long trajectories when exploring unknown environments. This limitation motivates the work we present here. Existing approaches display a trade-off between high success rate and long trajectories, with greedy decoding providing short, often incorrect paths ver-

sus the high success rates and long trajectories from beam search.

6. Conclusion

In this paper, we present FAST NAVIGATOR, a framework for using asynchronous search to boost any VLN navigator by enabling explicit backtrack when it gets lost. This framework can be easily plugged into current state-of-the-art agents to immediately improve their efficiency. Further, empirical results on the Room-to-Room dataset show that our agent achieves the state-of-the-art in Success Rate and SPL. Our search-based method can be easily extended to a more challenging settings, in which an agent might be given a goal without any route instruction [6, 12], or a complicated real visual environment [7].

References

- [1] P. Anderson, A. Chang, D. S. Chaplot, A. Dosovitskiy, S. Gupta, V. Koltun, J. Kosecka, J. Malik, R. Mottaghi, M. Savva, and A. Zamir. On evaluation of embodied navigation agents. *arXiv preprint arXiv:1807.06757*, 2018. 2, 5
- [2] P. Anderson, Q. Wu, D. Teney, J. Bruce, M. Johnson, N. Stünderhauf, I. Reid, S. Gould, and A. van den Hengel. Vision-and-language navigation: Interpreting visually-grounded navigation instructions in real environments. In *Proceedings of the IEEE Conference on Computer Vision and Pattern Recognition (CVPR)*, volume 2, 2018. 1, 2, 5, 8
- [3] S. Antol, A. Agrawal, J. Lu, M. Mitchell, D. Batra, C. Lawrence Zitnick, and D. Parikh. Vqa: Visual question answering. In *Proceedings of the IEEE international conference on computer vision*, pages 2425–2433, 2015. 8
- [4] C. Burges, T. Shaked, E. Renshaw, A. Lazier, M. Deeds, N. Hamilton, and G. Hullender. Learning to rank using gradient descent. In *Proceedings of the 22nd international conference on Machine learning*, pages 89–96. ACM, 2005. 10
- [5] A. Chang, A. Dai, T. Funkhouser, M. Halber, M. Nießner, M. Savva, S. Song, A. Zeng, and Y. Zhang. Matterport3d: Learning from rgb-d data in indoor environments. *arXiv preprint arXiv:1709.06158*, 2017. 5
- [6] D. S. Chaplot, K. M. Sathyendra, R. K. Pasumarthi, D. Rajagopal, and R. Salakhutdinov. Gated-attention architectures for task-oriented language grounding. *arXiv preprint arXiv:1706.07230*, 2017. 9
- [7] H. Chen, A. Shur, D. Misra, N. Snively, and Y. Artzi. Touchdown: Natural language navigation and spatial reasoning in visual street environments. *arXiv preprint arXiv:1811.12354*, 2018. 9
- [8] A. Das, S. Datta, G. Gkioxari, S. Lee, D. Parikh, and D. Batra. Embodied question answering. In *Proceedings of the IEEE Conference on Computer Vision and Pattern Recognition (CVPR)*, volume 5, page 6, 2018. 8
- [9] H. de Vries, K. Shuster, D. Batra, D. Parikh, J. Weston, and D. Kiela. Talk the walk: Navigating new york city through grounded dialogue. *arXiv preprint arXiv:1807.03367*, 2018. 8
- [10] D. Fried, R. Hu, V. Cirik, A. Rohrbach, J. Andreas, L.-P. Morency, T. Berg-Kirkpatrick, K. Saenko, D. Klein, and T. Darrell. Speaker-follower models for vision-and-language navigation. *arXiv preprint arXiv:1806.02724*, 2018. 1, 2, 5, 8
- [11] D. Gordon, A. Kembhavi, M. Rastegari, J. Redmon, D. Fox, and A. Farhadi. Iqa: Visual question answering in interactive environments. *arXiv preprint arXiv:1712.03316*, 1, 2017. 8
- [12] K. M. Hermann, F. Hill, S. Green, F. Wang, R. Faulkner, H. Soyer, D. Szepesvari, W. M. Czarnecki, M. Jaderberg, D. Teplyashin, et al. Grounded language learning in a simulated 3d world. *arXiv preprint arXiv:1706.06551*, 2017. 9
- [13] C.-Y. Ma, J. Lu, Z. Wu, G. AlRegib, Z. Kira, R. Socher, and C. Xiong. Self-aware visual-textual co-grounded navigation agent. In *International Conference on Learning Representations*, 2019. 1, 2, 5, 8, 11, 12, 13
- [14] H. Mei, M. Bansal, and M. R. Walter. Listen, attend, and walk: Neural mapping of navigational instructions to action sequences. In *AAAI*, volume 1, page 2, 2016. 8
- [15] P. Mirowski, R. Pascanu, F. Viola, H. Soyer, A. J. Ballard, A. Banino, M. Denil, R. Goroshin, L. Sifre, K. Kavukcuoglu, et al. Learning to navigate in complex environments. *arXiv preprint arXiv:1611.03673*, 2016. 8
- [16] D. Misra, A. Bennett, V. Blukis, E. Niklasson, M. Shatkhin, and Y. Artzi. Mapping instructions to actions in 3d environments with visual goal prediction. *arXiv preprint arXiv:1809.00786*, 2018. 8
- [17] D. Misra, J. Langford, and Y. Artzi. Mapping instructions and visual observations to actions with reinforcement learning. *arXiv preprint arXiv:1704.08795*, 2017. 8
- [18] J. Pearl. Heuristics: intelligent search strategies for computer problem solving. 1984. 8
- [19] M. Ranzato, S. Chopra, M. Auli, and W. Zaremba. Sequence level training with recurrent neural networks. *arXiv preprint arXiv:1511.06732*, 2015. 1
- [20] S. J. Russell and P. Norvig. *Artificial intelligence: a modern approach*. Malaysia; Pearson Education Limited,, 2016. 8
- [21] I. Sutskever, O. Vinyals, and Q. V. Le. Sequence to sequence learning with neural networks. In *Advances in neural information processing systems*, pages 3104–3112, 2014. 1
- [22] X. Wang, Q. Huang, A. Celikyilmaz, J. Gao, D. Shen, Y.-F. Wang, W. Y. Wang, and L. Zhang. Reinforced cross-modal matching and self-supervised imitation learning for vision-language navigation. *arXiv preprint arXiv:1811.10092*, 2018. 8
- [23] X. Wang, W. Xiong, H. Wang, and W. Y. Wang. Look before you leap: Bridging model-free and model-based reinforcement learning for planned-ahead vision-and-language navigation. *arXiv preprint arXiv:1803.07729*, 2018. 2, 8
- [24] Y. Zhu, R. Mottaghi, E. Kolve, J. J. Lim, A. Gupta, L. Fei-Fei, and A. Farhadi. Target-driven visual navigation in indoor scenes using deep reinforcement learning. In *Robotics and Automation (ICRA), 2017 IEEE International Conference on*, pages 3357–3364. IEEE, 2017. 8

A. Supplementary Material

Our appendix is structured to provide corresponding qualitative examples for the quantitative results in the paper, and additional implementation details for replication.

A.1. Qualitative comparison

Figures A1 through A3 show three examples comparing our approach to the previous state-of-the-art. In addition, the following URL includes a 90 second video <https://youtu.be/ik9uz06Fcpk> showing the first-person view of several agents navigating the environment with corresponding birds-eye-view maps.

A.2. Candidate Reranker

Given a collection of candidate trajectories, our reranker module assigns a score to each of the trajectories. The highest scoring trajectory is selected for the FAST agent’s next step. In our implementation, we use a 2-layer MLP as the reranker. We train the neural network using pairwise cross-entropy loss [4].

As input to the reranker, we concatenate the following features to obtain a 6-dimensional vector:

- sum of score logits for actions on the trajectory,
- mean of score logits for actions on the trajectory,
- sum of log probabilities for actions on the trajectory,
- mean of log probability for actions on the trajectory,
- progress monitor score for the completed trajectory
- speaker score for the completed trajectory

We feed the 6-dimensional vector through an *MLP*: $\text{BN} \rightarrow \text{FC} \rightarrow \text{BN} \rightarrow \text{Tanh} \rightarrow \text{FC}$, where BN is a layer of Batch Normalization, FC is a Fully Connected layer, and Tanh is the nonlinearity used. The first FC layer transforms the 6-dimensional input vector to a 6-dimensional hidden vector. The second FC layers project the 6-dimensional vector to a single floating-point value, which is used as the score for the given partial trajectory.

To train the *MLP*, we cache the candidate queue after running FAST for 40 steps. Each candidate trajectory in the queue has a corresponding score s_i . To calculate the loss, we minimize the pairwise cross-entropy loss:

$$-(s_1 - s_2) + \log(1 + \exp(s_1 - s_2))$$

where s_1 is the score for a good candidate and s_2 is the score of a bad candidate. We define good candidate trajectories as those that end within 3 meters of ground truth destination. In our cached training set, we have 4,378,729 pairs of training data. We train using a batch size of 3600, SGD optimizer with learning rate $5e^{-5}$ and momentum 0.6, and train for 30 epochs.

Instructions: Walk towards the television, turn around and walk down the stairs directly to your left. Stop directly at the bottom of the stairs.

























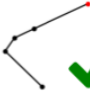












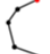











T	Ground Truth	SMNA	FAST
1	 	 	 
2	 	 	 
3	 	 	 
4	 	 	 
5	  	 	 
6		 	 
7		 	 
8		 	  
⋮		 	
24		  	

Figure A1. Comparison of the previously state-of-the-art SMNA model [13] to our FAST NAVIGATOR method, with the ground truth as reference. Note how SMNA retraces its steps multiple times due to lack of global information. This example is taken from Room-to-Room, path 2617, instruction set 2. You can view a video of this trajectory here: <https://youtu.be/ik9uz06Fcpk>.

Instructions: Walk out of the bedroom through the open door into the hallway. Turn the corner and walk into the dining area. Pass the dining table and walk into the living room area towards the television. Stop near the chair and open sliding doors to outside.














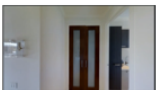
























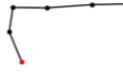





T	Ground Truth	SMNA	FAST
1	 	 	 
2	 	 	 
3	 	 	 
4	 	 	 
5	 	 	 
6	 	 	 
7		 	 
8		 	 

Figure A2. Comparison of the previously state-of-the-art SMNA model [13] to our FAST NAVIGATOR method, with the ground truth as reference. Note how SMNA retraces its steps multiple times due to lack of global information. This example is taken from Room-to-Room, path 15, instruction set 1. You can view a video of this trajectory here: <https://youtu.be/ik9uz06Fcpk>.

Instructions: Walk towards the television, turn around and walk down the stairs directly to your left. Stop directly at the bottom of the stairs.












































T	Ground Truth	SMNA	FAST
1	 	 	 
2	 	 	 
3	 	 	 
4	 	 	 
5	 	 	 
6	  	  	 
7			 
8			  

Figure A3. Comparison of the previously state-of-the-art SMNA model [13] to our FAST NAVIGATOR method, with the ground truth as reference. Note how SMNA retraces its steps multiple times due to lack of global information. This example is taken from Room-to-Room, path 1759, instruction set 1. You can view a video of this trajectory here: <https://youtu.be/ik9uz06Fcpk>.